J. Biochem. **142,** 481–490 (2007)
doi:10.1093/jb/mvm161

Characterization of Native Myosin VI Isolated from Sea Urchin Eggs

Souhei Sakata[1], Yuuko Watanabe[1], Jiro Usukura[2] and Issei Mabuchi[1,*]

[1]Division of Biology, Department of Life Sciences, Graduate School of Arts and Science, University of Tokyo, Komaba, Meguro-ku, Tokyo 153-8902; and [2]Center for Cooperative Research in Advanced Science and Technology, Nagoya University, Nagoya, 464-0814, Japan

Received May 30, 2007; accepted July 16, 2007; published online August 30, 2007

Myosin VI is a molecular motor that is ubiquitously expressed among eukaryotic cells, and thought to be involved in membrane trafficking and anchoring the organelle to actin cytoskeleton. Studies on myosin VI have been carried out using recombinant proteins, but native myosin VI has not been purified yet. Here we purified native myosin VI from sea urchin eggs and characterized its properties. We found that the native myosin VI was a monomeric and non-processive motor protein, and also showed that it moved toward the pointed end of F-actin. Ca^{2+} stimulated actin-activated MgATPase activity of the native myosin VI, while it lowered its motility on F-actin. Immunofluorescence microscopy showed that the myosin VI was translocated from the inner cytoplasm to the cortex after fertilization. Myosin VI may be involved in endocytic activities in fertilized eggs.

Key words: F-actin, motor protein, myosin VI, sea urchin, unconventional myosin.

Abbreviations: NP-40, Nonidet P-40; PMSF, phenylmethylsulfonyl fluoride; PVDF, polyvinylydene difluoride; TAME, *N-p*-tosyl-L-arginine methyl ester.

Myosin is a motor protein that moves along an actin filament. There are so far 18 classes of myosins in the myosin superfamily based on phylogenetic sequence comparisons of the motor domains (*1*). Myosin VI was first identified in *Drosophila melanogaster* (*2*), and then found in mammals (*3*, *4*). In *Drosophila*, myosin VI is thought to play a role in formation of metaphase furrow in embryos (*5*) and is also involved in individualization of spermatids (*6*, *7*). Myosin VI plays a role in organization of stereocilia in the inner ear in mice: it is not expressed in *Snell's waltzer* mice (*3*) which are deaf because of a defect in formation of stereocilia (*8*). Another role suggested for myosin VI is a transport of endocytic vesicles. Myosin VI is co-localized with clathrin-coated vesicles, and its globular tail interacts with Disable 2 (Dab2, DOC-2) which is involved in endocytosis in cultured mammalian cells (*9–11*).

Based on analysis of its amino acid sequence, a myosin VI heavy chain has a motor (head) domain in the N-terminal half, an IQ motif, a coiled-coil domain and a globular tail domain at the C-terminus. It has been shown using recombinant myosin VI that the motor domain binds to an actin filament and moves on the filament to its pointed end being different from conventional myosin (*12*). The tail domain has been considered to bind a specific cargo such as the endocytic vesicles and play a role in transport of the cargo on the actin filament (*9–11*, *13*). Two calmodulins bind as light chains, one of which binds to the IQ motif and the other binds to a unique insert between the head domain and the IQ motif (*14*, *15*). Thus, the function of myosin VI may be regulated by Ca^{2+}.

It has been shown that recombinant chicken intestinal brush border myosin VI is a monomeric protein and also a non-processive motor (*16*). Myosin VI in normal rat kidney fibroblastic tissue cultured cells has also been suggested to behave as monomers since dimers have not been detected after treatment of the cell lysate with a chemical cross-linker (*16*). Non-processivity may not be adequate to transport a cargo, because a non-processive motor detaches from cytoskeleton during its ATPase cycle: the cargo will be released from actin cytoskeleton when myosin VI binds ATP and hydrolyses it. However, it has recently been reported that recombinant myosin VI is able to dimerize and the dimer behaves as a processive motor (*17*). This suggests a possibility that myosin VI may processively transport vesicles in a cell.

The ATPase activity and *in vitro* motility of recombinant myosin VI has also been investigated to some extent (*18*, *19*). These reports have shown that its ATPase activity is not significantly influenced by Ca^{2+} concentrations. However, its in vitro motility is dependent on Ca^{2+} concentrations such that it is increased with decreasing Ca^{2+} concentrations. Since these biochemical studies have been performed using mammalian recombinant myosin VI, it has been desirable to reinvestigate properties of myosin VI using a native protein.

We have previously searched for F-actin-binding proteins from sea urchin eggs using F-actin affinity column chromatography (*20*), and identified a 150 kDa protein to be myosin VI, which was eluted from the column with ATP. Here, we purified native myosin VI

*To whom correspondence should be addressed. Department of Chemistry, Gakushuin University, 1-5-1 Mejiro, Toshima-ku, Tokyo 171-8588. Tel: +81-3-3986-0221, ext. 6421, Fax: +81-3-5992-1029, E-mail: issei.mabuchi@gakushuin.ac.jp

using its F-actin-binding ability, characterized its biochemical properties and localized it in the egg.

MATERIALS AND METHODS

Preparation of a Sea Urchin Egg Extract—Unfertilized eggs of the sea urchins *Hemicentrotus pulcherrimus* and *Anthocidaris crassispina* were used. Egg extracts were prepared as described previously (*20*).

Purification of MyosinVI and MyosinII—Temperatures were kept at 0–4°C unless otherwise noted. Rabbit skeletal muscle myosin II and actin were prepared by the method of Weeds and Hartley (*21*) and Spudich and Watt (*22*), respectively. Actin was further purified through a Sephadex G-100 (Pharmacia Biotech, Uppsala, Sweden) column.

The egg extract was diluted 5-fold with buffer A (50 mM MOPS-KOH (pH 7.5), 10%(w/v) glycerol, 25 mM KCl, 5 mM $MgCl_2$, 5 mM EGTA, 0.05%(v/v) NP-40, 2 mM DTT, 2 mM TAME, 5 μg/ml leupeptin) and 50 mM glucose and 10 U/ml hexokinase were supplemented to hydrolyse ATP. Then, F-actin (25 mg) was added to the diluted extract (250 ml) and the extract was stirred gently for 20 min. Visible aggregates were formed in the extract. The aggregates were collected by centrifugation at 8,000*g* for 10 min, and dissolved in 4 ml buffer B [0.5 M KCl, 20 mM MOPS-KOH (pH 7.5), 10%(w/v) glycerol, 5 mM $MgCl_2$, 2 mM DTT, 5 mM EGTA, 2 mM TAME, 5 μg/ml leupeptin]. The solution was centrifuged at 8,000*g* for 10 min to remove insoluble materials. The supernatant was further ultracentrifuged at 260,000*g* for 30 min. The pellet was homogenized in 1 ml buffer B with a Teflon-glass homogenizer. This homogenate was again ultracentrifuged at 260,000*g* for 30 min, and the pellet was homogenized in 0.2 ml buffer B. Ten mM ATP and 5 mM $MgCl_2$ were added to the homogenate, and it was kept for 5 min at 4°C. The homogenate was ultracentrifuged at 260,000*g* for 30 min. The supernatant was loaded onto a Superose6 (Pharmacia Biotech, Uppsala, Sweden) gel filtration column pre-equilibrated with buffer B containing 1 mM ATP. Eluted fractions were analysed by SDS–PAGE, and those containing myosinVI were pooled.

Actin-activated MgATPase Activity—Actin-activated MgATPase activity was measured at 25°C in a solution of 25 mM imidazole (pH 7.5), 50 mM KCl, 4 mM $MgCl_2$, 1 mM DTT, 1 mM EGTA, 20 units/ml pyruvate kinase and 2 mM phosphoenol pyruvate with 20 nM purified myosin VI. Liberated Pi was determined by the Malachite Green method (*23*).

In Vitro Motility Assay—In vitro motility assay was performed according to the method described by Kron and Spudich (*24*) with modifications. The antibodies against myosin VI globular tail was used to tether myosin VI onto a nitrocellulose-coated glass coverslip. A flow chamber made with the coverslip and a glass slide was successively filled and incubated for 5–10 min at room temperature with the antibodies whose concentration was 0.1 mg/ml, 1 mg/ml bovine serum albumin to block non-specific binding of proteins and 50 μg/ml purified myosin VI. After washing out the excess myosin VI, the chamber was filled with rhodamine-phalloidin-labelled F-actin, and the excess F-actin was washed out with a solution of 25 mM imidazole (pH 7.5), 50 mM KCl, 5 mM $MgCl_2$, 1 mM DTT and 1 mM EGTA containing 18 μg/ml catalase, 0.1 mg/ml glucose oxidase and 3.0 mg/ml glucose to reduce photobleaching. Sliding velocity was measured at 22°C.

The landing rate of F-actin on myosin VI attached on a glass surface and the duty ratio of myosin VI were estimated according to Hancock and Howard (*25*) and Uyeda *et al*. (*26*), respectively. Concentration of myosin VI was varied from 20 to 0.2 μg/ml. Densities of myosin VI on the nitrocellulose-coated glass surface were determined by estimating concentration of unbound myosin VI and the area of the glass surface.

Expression of Myosin VI Globular Tail Domain—A DNA fragment coding for the globular tail domain of *H. pulcherrimus* myosin VI was generated by polymerase chain reaction (PCR) using 5′-primer (5′-GGAATTCG AAGAAGAACAACGTAGAAGG-3′) with a *Eco*RI linker, a 3′-primer (5′-GTCGACATCAACGAGCTTTCAAGCTC TGCG-3′) with *Sal*I linker, and a cDNA pool of *H. pulcherrimus* (Yonemura, I. and Mabuchi, I., unpublished observations) as the template. These primers were designed according to nucleotide sequence of the myosin VI gene of *Strongylocentrotus purpuratus* (*27*). The PCR product was subcloned into *Eco*RI- and *Sal*I-treated pUC119 (Takara Bio Inc., Otsu, Japan) and sequenced using a Genetic analyser 310 (Applied Biosystems, Foster City, CA, USA). The deduced amino acid sequence showed 96% identity with 1012–1267 aa of *S. purpuratus* myosin VI. The generated DNA fragment was subcloned into pGEX4T-1 (Pharmacia Biotech, Uppsala, Sweden) to express a glutathione-s-transferase fusion protein, which was isolated with a glutathione-Sepharose 4B (Pharmacia Biotech) column and eluted by digesting with thrombin.

Antibodies—Polyclonal antibodies against the myosin VI globular tail domain was raised in a rabbit, and affinity-purified using the antigen immobilized on Affi-Gel 10 (Bio-Rad Labs, Hercules, CA, USA). Antibodies against a peptide IDENRKV of myosin VI named pAb were also raised in a rabbit. This peptide corresponds to 2–8 aa of *S. purpuratus* myosin VI. pAb was affinity-purified using myosin VI on a PVDF membrane. The mouse monoclonal antibody to calmodulin was a gift from Dr Megumi Moriya (Hokkaido University, Sapporo, Japan).

Preparation of Doubly Labelled F-actin—To determine the direction of sliding of myosin VI on F-actin in *in vitro* motility assay, we made doubly labelled F-actin whose pointed end was brighter than its barbed end. F-actin (0.79 μM) was labelled with an equal molar of rhodamine-phalloidin (Fluka AG, Switzerland) overnight on ice in F-actin-labelling buffer (25 mM imidazole (pH 7.5), 50 mM KCl, 5 mM $MgCl_2$, 1 mM EGTA, 1 mM DTT). The labelled F-actin was diluted with F-actin-labelling buffer to give a concentration of 0.24–0.48 μM and then G-actin (0.2–0.5 μM) was added to polymerize at the barbed end of the F-actin together with a 1 : 4 mixture of rhodamine-phalloidin and phalloidin (Sigma, St Louis, MO,USA) (total phalloidin (rhodamine-phalloidin plus phalloidin) concentration, 0.2–0.5 μM). The mixture was kept overnight in the dark.

Table 1. **Summary of purification of myosin VI from sea urchin eggs.**

Fractions	Conc. of protein (mg/ml)	Volume (ml)	Total protein (mg)	Content[a] of myosin VI (%)	Recovery (%)
Extract	34	50	1,700	ND	ND
Extract + F-actin	7.0	250	1,750	ND	ND
Aggregates	6.7	7.0	47	1.0[b]	100
Pellets after ultracentrifugation	45	0.2	9	3.0[b]	57
ATP-soluble fraction	2.2	0.15	0.33	23[b]	16
Superose6	0.13	0.40	0.054	95[c]	11

The purification was started with 12 ml packed unfertilized sea urchin eggs and was carried out as described in 'Materials and Methods'.
[a]Content of myosin VI was estimated by densitometric analysis. [b]The values were estimated for myosin VI heavy chain. [c]The value was estimated for heavy chain plus light chain. ND, not determined.

Electron Microscopy—Purified myosin VI was dialysed against a solution of 25 mM imidazole (pH 7.5), 10% (w/v) glycerol, 50 mM KCl, 4 mM $MgCl_2$, 1 mM DTT, 1 mM EGTA. Then, glycerol was added to give 50% (v/v), and myosin VI was rotary-shadowed as described previously (*28*). Specimens were examined with an JEM 1200EX (JEOL Ltd., Tokyo, Japan) electron microscope at an accelerating voltage of 80 kV.

Immunoprecipitation—Immunoprecipitation was carried out using the antibodies against myosin VI globular tail. Protein G Sepharose™ beads (Pharmacia Biotech, Uppsala, Sweden) were added to an antibody solution and then purified myosin VI was further added. The mixture was agitated overnight at 4°C. The beads were collected by centrifugation at 3,000*g* for 5 min, and washed with 25 mM imidazole (pH 7.5), 50 mM KCl, 4 mM $MgCl_2$, 1 mM DTT and 1 mM EGTA-Ca buffer. The beads were dissolved in the sample buffer for SDS–PAGE and analysed by SDS–PAGE.

Immunofluorescence Microscopy—Indirect immunofluorescence microscopy was carried out according to Mabuchi (*29*). Eggs of *H. pulcherrimus* were attached onto a protamine(10 mg/ml)-coated glass slide. For staining of whole eggs, the eggs were fixed for 10 min at room temperature with 5% (v/v) formalin dissolved in F-buffer [0.1 M KCl, 2 mM $MgCl_2$, 1 mM EGTA, 10 mM MOPS-KOH (pH 7.4) for fertilized eggs or 10 mM PIPES-KOH (pH 6.8) for unfertilized eggs] containing 0.8 M glucose (glucose-F-buffer). They were further incubated for 40 min with glucose-F-buffer containing 5% formalin and 0.5% (v/v) NP-40. They were washed with F-buffer containing 0.8 M glycerol (glycerol-F-buffer) and incubated with pAb for 2 h. They were washed with glycerol-F-buffer and incubated with rhodamine-conjugated goat anti-rabbit IgG (Cooper Biomed. Inc., Malvern, PA, USA) for 2 h. Cortices were isolated on a protamine-coated glass slide and processed in the same manner as described above. Specimens were examined with an Axioscope fluorescence microscope (Carl Zeiss, Tokyo, Japan) equipped with a Plan Neofluar 63× objective lens.

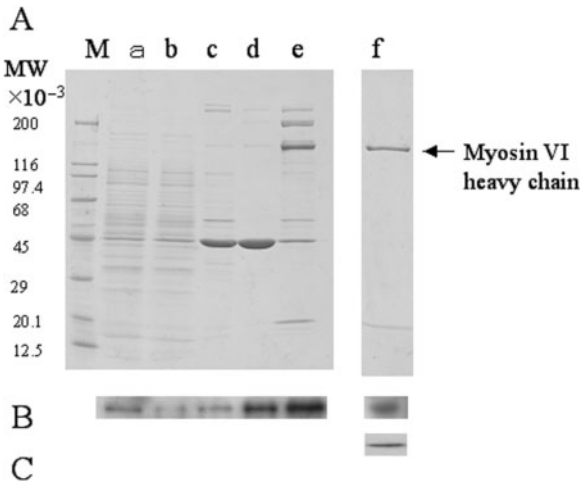

Fig. 1. **Purification of myosin VI from sea urchin eggs.** (A) Myosin VI-containing fractions during purification of myosin VI (see 'MATERIALS AND METHODS' section) were analysed by SDS–PAGE and CBB staining. Lane (a): unfertilized sea urchin extract; (b): the extract supplemented with F-actin; (c): aggregates formed upon addition of F-actin; (d): pellets after ultracentrifugation from 0.5 M KCl-solubilized aggregates; (e): the ATP-soluble fraction obtained from (d); (f): purified myosin VI. The equal amount of protein was loaded from lanes (a) to (e). Lane (M) represents molecular weight makers. (B, C) Western blotting analyses of myosin-VI-containing fractions during the purification of myosin VI. (B) Detection with antibodies against myosin VI tail. Only the 150 kDa position is shown; (C) detection with anti-calmodulin monoclonal antibody. Only the calmodulin band is shown.

RESULTS

Purification of Native Myosin VI From Sea Urchin Eggs—Myosin VI heavy chain was detected in the unfertilized sea urchin egg extract as a 150 kDa band (Fig. 1). We isolated the native myosin VI from the extract by co-precipitation with exogenously added F-actin. We found that aggregates were formed within a few minutes after addition of F-actin to the extract at 0°C, which was enriched with myosin VI as judged by western blotting using the antibodies against the globular tail of sea urchin myosin VI. Myosin VI was solubilized with F-actin from the aggregates with 0.5 M KCl, further separated from F-actin by the addition of ATP and Mg^{2+}, and finally purified by a gel filtration column chromatography [Fig. 1A lane (f)]. A 200 kDa protein which probably represented myoin II heavy chain was removed from the myosin VI fraction by the gel filtration column chromatography. The purified myosin VI fraction contained the 150 kDa main component and a 20 kDa minor component. The 20 kDa protein was revealed to be calmodulin by western blotting using the anti-calmodulin antibody (Fig. 1C), which is likely to be a light chain of myosin VI. We typically obtained about 50 μg native myosin VI from 12 ml packed sea urchin eggs (Table 1).

Estimation of the Molecular Weight of Native Myosin VI—We estimated the molecular weight of native myosin VI using a gel filtration column chromatography (Fig. 2A) to be 183 k. The molecular weight of sea

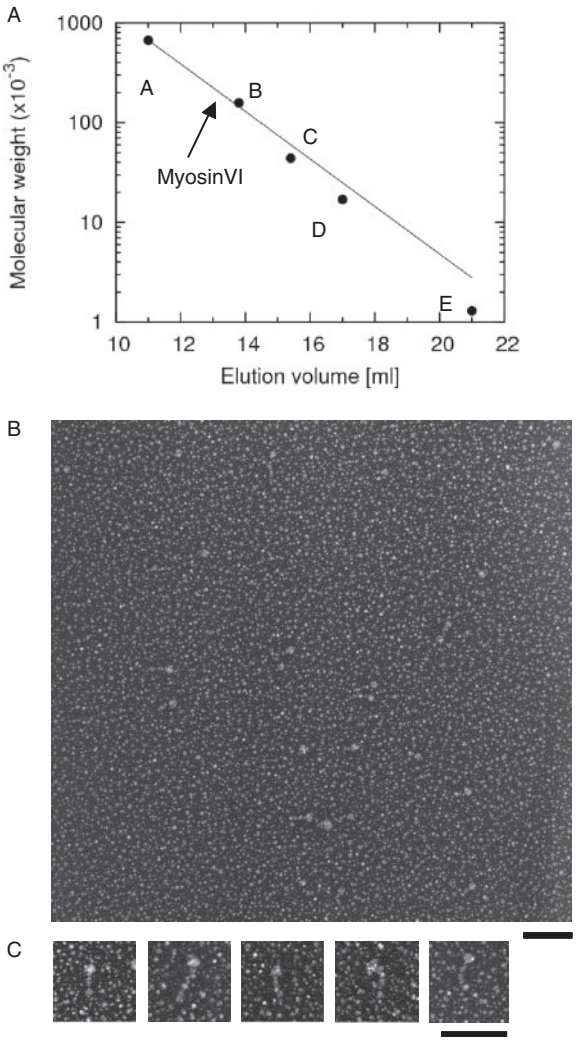

Fig. 2. **Native myosin VI is a monomeric protein.** (A) The calibration curve obtained using the Superose6 gel filtration column. The column was equilibrated with 25 mM MOPS-KOH(pH 7.5), 10%(w/v)glycerol, 50 mM KCl, 5 mM $MgCl_2$, 2 mM EGTA, 1 mM ATP, 2 mM DTT, 2 mM TAME and 5 μg/ml leupeptin. The ATP-soluble fraction (see 'MATERIALS AND METHODS' section) was dialysed against the equilibration buffer and ultracentrifuged and loaded onto the column. The standard proteins used were; A, thyroglobulin (670 k); B, γ-globulin (158 k); C, ovalbumin (44 k); D, myoglobin (17 k); and E, vitamin B-12 (1.35 k). The elution position of myosin VI is indicated by an arrow, giving a molecular weight of 183.3 k. (B,C) Electron micrographs of rotary-shadowed myosin VI. Bars, 100 nm.

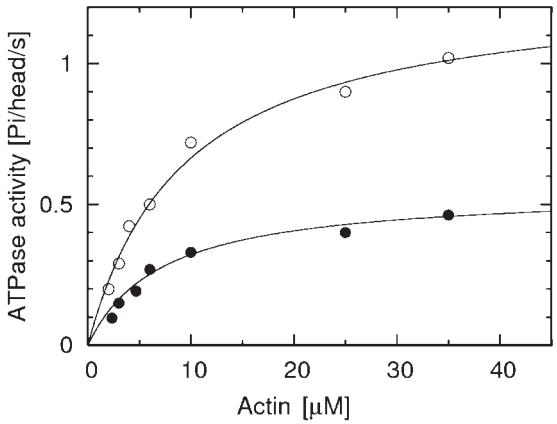

Fig. 3. **F-actin dependency of actin-activated MgATPase activity of native myosin VI.** Actin-activated MgATPase activity of myosin VI was measured using a reaction solution of 25 mM imidazole (pH 7.5), 50 mM KCl, 4 mM $MgCl_2$, 1 mM DTT, 1 mM ATP and 20 nM myosin VI at 25°C in the presence of either 1 mM EGTA (closed circles) or 1 mM $CaCl_2$ (open circles). *Solid lines* are fitting curves based on the Michaelis–Menten equation $V = V_{max}\cdot[action]/(K_{actin} + [actin])$.

Table 2. **Summary of actin-activated MgATPase activity of native myosin VI.**

	$V^{max}_{actin}[head^{-1}s^{-1}]$	$K_{actin}[\mu M]$	$V^{max}_{ATP}[head^{-1}s^{-1}]$	$K_{ATP}[\mu M]$
EGTA	0.67 ± 0.16	9.2 ± 4.3	0.76 ± 0.14	480 ± 80
pCa3	1.1 ± 0.2	7.0 ± 2.2	1.3 ± 0.10	360 ± 120

The values of both V_{max} and K_M were calculated by fitting the data of MgATPase activity to the Michaelis–Menten equation. The assays were performed at 25°C in 25 mM imidazole(pH 7.5), 50 mM KCl, 4 mM $MgCl_2$, 1 mM DTT, 1 mM EGTA or 1 mM $CaCl_2$ and 20 nM myosin VI. F-actin dependency or ATP dependency of the MgATPase activity was measured with 1 mM ATP or 20 μM F-actin, respectively.

urchin myosin VI heavy chain predicted from the amino acid sequence is 146 k (*27*). Assuming that two calmodulins bind to one myosin VI heavy chain, the predicted molecular weight is about 180 k, which agrees well with that estimated here. This result suggests that the purified native sea urchin myosin VI is monomeric as to its heavy chain.

Electron Microscopy of Native Myosin VI—Electron micrographs of rotary shadowed native myosin VI specimen revealed that the molecule consisted of a globular part and a straight tail extended from the globular part (Fig. 2B and C). In some images, the end of the tail seemed to be bulged. Probably, the larger globular part represents the motor domain and the bulge represents the globular tail domain. The mean total length of the molecule was 54.8 ± 11.3 nm ($n = 55$). The appearance of native myosin VI suggested that it is monomeric as to its heavy chain that is consistent with the estimation from the gel filtration column chromatography.

Actin-activated MgATPase Activity of Myosin VI—Figure 3 shows F-actin concentration dependency of actin-activated MgATPase activity of native myosin VI. The MgATPase activity was activated by F-actin. The data fitted the Michaelis–Menten equation. Estimated K_{actin}, V^{max}_{actin}, K_{ATP} and V^{max}_{ATP} are shown in Table 2. Both V^{max}_{actin} and V^{max}_{ATP} were apparently stimulated about 2-fold in the presence of high concentration of Ca^{2+}. The addition of exogenous calmodulin did not affect the MgATPase activity in the presence of 1 mM $CaCl_2$ (data not shown).

Next, the actin-activated MgATPase activity was measured as a function of free Ca^{2+} concentration. It was stimulated by free Ca^{2+} (Fig. 4A). The stimulation of actin-activated MgATPase activity by Ca^{2+} has also been

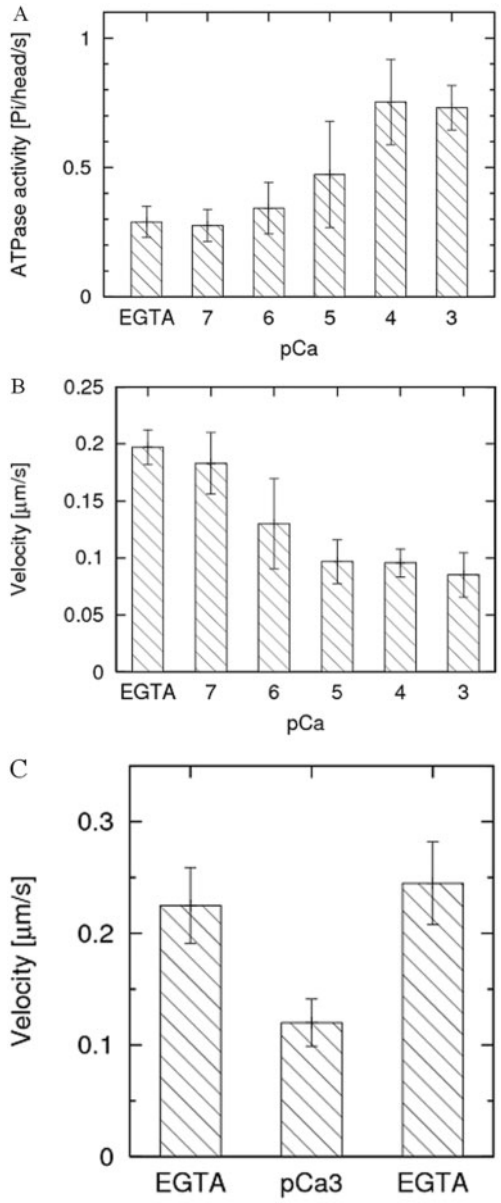

Fig. 4. **The effect of Ca^{2+} on actin-activated MgATPase activity and motile activity of native myosin VI.** (A) The pCa dependency of actin-activated MgATPase activity. ATPase activity was measured in a solution of 25 mM imidazole (pH 7.5), 50 mM KCl, 4 mM $MgCl_2$, 1 mM DTT, 1 mM ATP, 20 μM F-actin, 20 nM myosin VI and 1 mM EGTA-Ca buffer. Actin-activaed MgATPase activity was stimulated by high concentrations of free Ca^{2+}. (B) The pCa dependency of sliding velocity of F-actin. Motility assay was carried out in 25 mM imidazole (pH 7.5), 50 mM KCl, 5 mM $MgCl_2$, 1 mM EGTA, 1 mM DTT, 1 mM ATP and $CaCl_2$ was added to adjust pCa. These data are shown as mean ± SD of two or three separate preparations of myosin VI. (C) Suppression of the sliding velocity by Ca^{2+} was reversible. The motility assay was first carried out in 1 mM EGTA in the same buffer solution as described in (B), and the flow chamber was washed five times and perfused with the assay buffer of pCa 3. After measuring the sliding velocity at pCa 3, the chamber was washed five times and perfused with the assay buffer plus 1 mM EGTA and then the sliding velocity was measured.

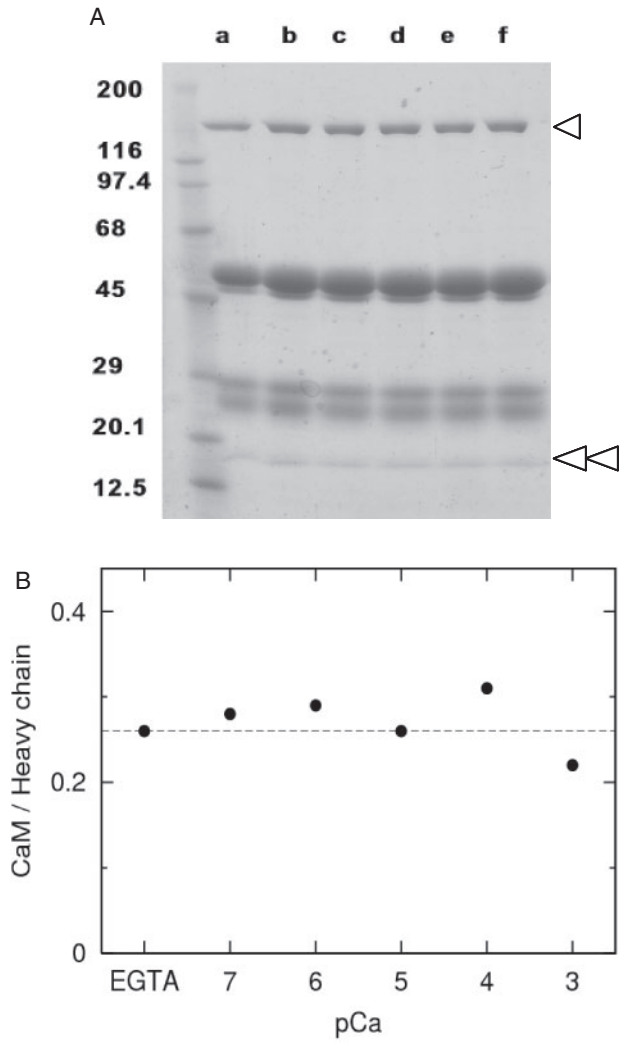

Fig. 5. **Calmodulin does not dissociate from myosin VI heavy chain in the presence of Ca^{2+}.** (A) Purified myosin VI was immunoprecipitated by the antibodies against myosin VI globular tail. The lanes contain the immunoprecipitates washed with excess 1 mM EGTA (a), pCa 7 buffer (b), pCa 6 buffer (c), pCa 5 buffer (d), pCa 4 buffer (e) or pCa 3 buffer (f). single arrowhead, myosin VI heavy chain, double arrowheads, calmodulin. The thick bands around 50 kDa represent IgG heavy chains, and the bands around 25 kDa are IgG light chains. (B) The densitometric analysis of myosin VI heavy chains and calmodulins. The density of calmodulin band was divided by that of myosin VI heavy chain.

found for myosin V and myosin I. In both cases, calmodulins dissociates from the heavy chains at high Ca^{2+} concentrations (*30*, *31*). On the other hand, calmodulin does not dissociate from the heavy chain in mammalian myosin VI at high Ca^{2+} concentrations, and the MgATPase activity was not affected by Ca^{2+} (*18*, *19*). Thus, we examined whether calmodulin dissociates or not in native myosin VI. Purified native myosin VI was immunoprecipitated with antibodies against myosin VI globular tail, and washed with solutions containing various free Ca^{2+} concentrations. Then the immunoprecipitates were analysed by SDS–PAGE (Fig. 5A).

As shown in Fig. 5B, the densitometric analysis revealed that the amount of calmodulin bound to myosin VI heavy chain did not change upon changing free Ca^{2+} concentration. This result indicated that calmodulin did not dissociate from the native myosin VI heavy chains at low or high concentrations of free Ca^{2+}.

In Vitro Motility Assay of Myosin VI—To evaluate the motor activity of native myosin VI more directly, purified native myosin VI was subjected to *in vitro* motility assay. In this assay, the purified myosin VI was attached onto a nitrocellulose membrane via antibodies against its globular tail. Figure 4B shows effect of free Ca^{2+} concentration on the motility of F-actin. Sliding velocity was lowered at high free Ca^{2+} concentrations. In addition, the motility assay was performed using the same flow chamber by changing free Ca^{2+} concentration in the absence of exogenous calmodulin. The chamber solution was changed from 1 mM EGTA to 1 mM $CaCl_2$ and then returned to 1 mM EGTA again (Fig. 4C). Sliding velocity was first high in EGTA, then lowered at pCa 3, and then restored again in EGTA. This result suggested that the low sliding velocity in the presence of Ca^{2+} was not due to dissociation of calmodulin from the heavy chain, and was consistent with the above result that the calmodulin binding was not afected by free Ca^{2+} concentration.

The Direction of Movement of Native Myosin VI on the F-actin—It has been shown that mammalian recombinant myosin VI is a minus end-directed motor (*12*). We used doubly labelled F-actin whose pointed-end was labelled brighter than the barbed end in the *in vitro* motility assay to determine the direction of movement of native myosin VI on the F-actin. As shown in Fig. 6A, the darker end was the leading end when the F-actin moved on the native myosin VI. Figure 6B summarizes the results of the assay. The majority of F-actin moved with the darker end lead at the rate of ~0.1 μm/s. This is contrasted with the movement of F-actin on rabbit skeletal myosin II which translocated F-actin with the brighter end lead at the rate of 2–3 μm/s. This means that native myosin VI slowly moves toward the pointed end of F-actin-like recombinant porcine myosin VI (*12*).

The Processivity of Native Myosin VI—It has previously been reported that double-headed recombinant myosin VI is a processive motor (*32*). On the other hand, single-headed myosin VI has been reported to be a non-processive motor (*16*). To examine the processivity of native myosin VI, we estimated both the landing rate of F-actin and the sliding velocity as functions of myosin VI density on the coverslip surface. By fitting the data of the landing rate to the equation $L(\rho) = Z(1 - \exp(-\rho A))^n$ where L is the landing rate, ρ is the density of myosin VI on a coverslip, Z is the maximum landing rate, A is the mean area where one motor protein interacts with surounding F-actin, and n is the number of myosin VI molecules required for binding and continuous sliding of F-actin (*25*), we obtained the value $n = 2.08$ (Fig. 7A). This analysis indicated that at least two myosin VI heads were required for the successful sliding event. Next, dependency of sliding velocity of F-actin on the density of myosin VI was examined. It is known that the sliding velocity of F-actin decreases when the surface density of a non-processive motor (*26*), such as myosin II, is decreased, whereas the velocity is not affected by the density of processive motors. The velocity became slower as the myosin VI density was lowered (Fig. 7B). This indicated that the native monomeric myosin VI is a non-processive motor.

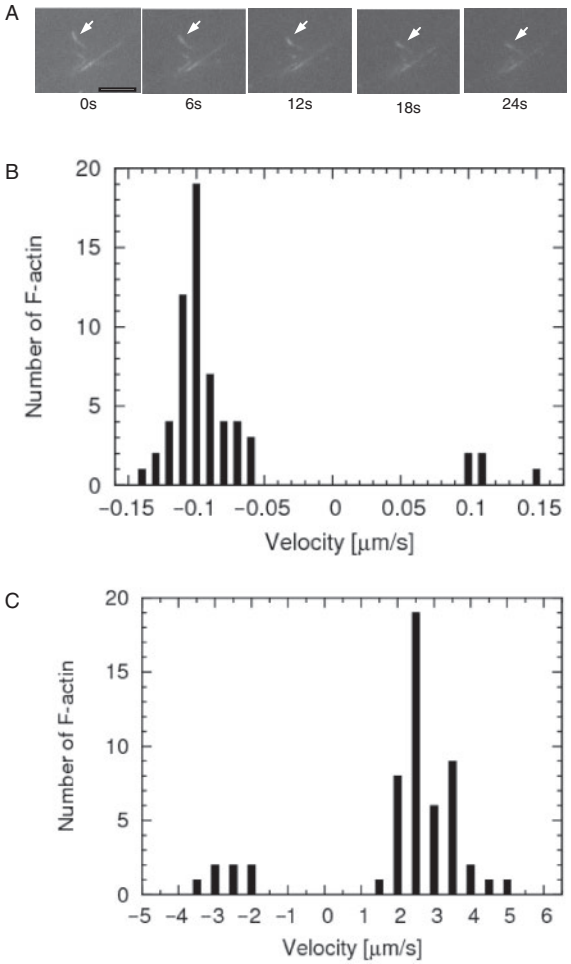

Fig. 6. **Native monomeric myosin VI moves towards the pointed end of F-actin.** (A) The doubly labelled F-actin is translocated on the native myosin VI. The arrow indicates the doubly labelled and sliding F-actin. The brighter end was the pointed end of F-actin. *In vitro* motility assay was carried out in the presence of 1 mM EGTA without added Ca^{2+}, and other assay conditions were the same as those described in the legend of Fig. 4B. Bar, 5 μm. (B) and (C) Relation between velocity and population of F-actin moved on native myosin VI (B) or rabbit skeletal myosin II (C), respectively. Moved F-actin whose leading end was the barbed end has a negative sign on the velocity value.

Immunofluorescent Localization of Myosin VI in Sea Urchin Eggs—To examine the localization of myosin VI in sea urchin eggs, both unfertilized eggs and fertilized eggs were stained with the antibody pAb (Fig. 8). Figure 8A shows that pAb was able to detect myosin VI with a high specificity. A punctate staining was observed in the cytoplasm of unfertilized eggs with pAb, while no staining was observed using control IgG (Fig. 8B and C). At 30 min after fertilization, the staining of the cytoplasm

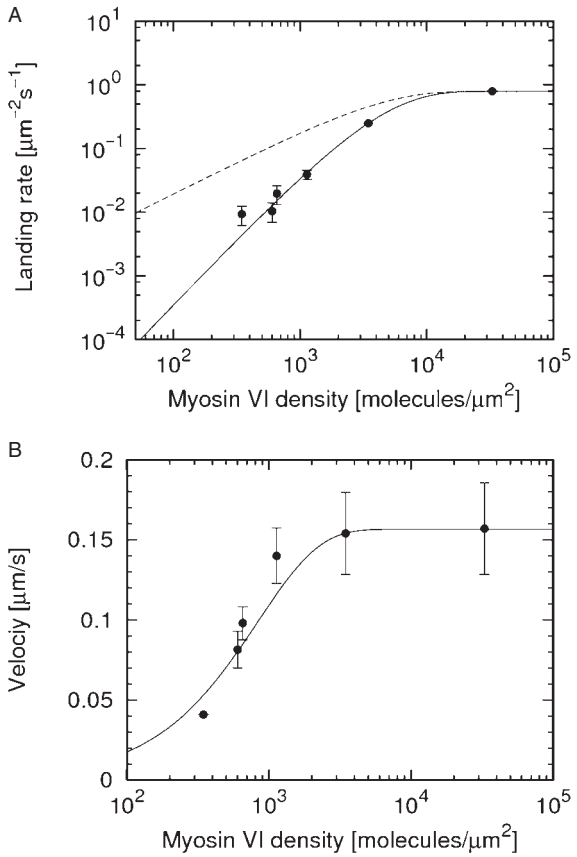

Fig. 7. **Monomeric native myosin VI is a non-processive motor.** (A) The plot of landing rate of F-actin versus myosin VI density on the unit surface area. The data were fitted to the equation: $L(\rho) = Z(1 - \exp(-\rho A))^n$ where L is the landing rate; Z is the maximum landing rate; n is the number of myosin molecules required for binding and continuous sliding of F-actin (*25*). We obtained values for the parameters: $Z = 0.794\,\mu m^{-1}\,s^{-1}$, $A = 0.00025\,\mu m^2$ and $n = 2.08$. The *dashed line* and *solid line* represent theoretical lines where $n = 1$ and $n = 2.1$, respectively. (B) Plot of F-actin sliding velocity versus myosin VI density on the unit surface area. Using the equation: $V(\rho) = V_{max}(1 - (1 - f)^{\rho A})$ (*27*), we obtained following values: $V_{max} = 0.157$ μm/s, $A = 0.0017\,\mu m^2$, $f = 0.495$. The *solid line* represents the theoretical line. Data obtained using two different preparations of myosin VI are plotted in both (A) and (B). Each value is shown as mean ± SD.

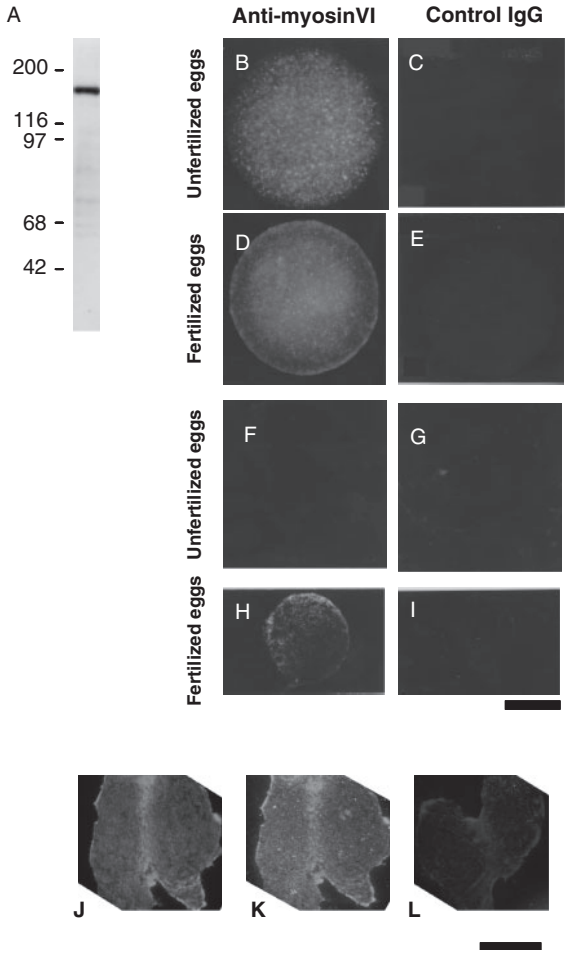

Fig. 8. **Immunofluorescence microscopy of *H. pulcherrimus* eggs.** (A) Western blotting of unfertilized egg extract with pAb. (B, C) Unfertilized eggs; (D, E) fertilized eggs 30 min after fertilization; (F, G) cortices isolated from unfertilized eggs; (H, I) cortices isolated from fertilized eggs; (J, K, L) cortices containing the contractile ring isolated from dividing eggs; (B, D, F, H and K) stained with affinity-purified pAb. (C, E, G, I and L), Stained with pre-immune IgG. (J) Stained with rhodamine-phalloidin. Bars, 50 μm.

decreased while the cortical layer was clearly stained (Fig. 8D and E). Next we isolated and stained the cortices from unfertilized or fertilized sea urchin eggs (Fig. 8F–I). Although no staining was seen in the unfertilized egg cortex, a network-like staining was seen in the cortices of fertilized eggs 30 min after fertilization. During cleavage, actin filaments were concentrated in the cleavage furrow and oriented in parallel to the cleavage plane to form the contractile ring (Fig. 8J). Myosin VI was also concentrated in this region (Fig. 8K).

DISCUSSION

Purification of Native Myosin VI from Sea Urchin Eggs—We purified native myosin VI for the first time from sea urchin eggs. This allowed us to characterize it and compare the properties with those of recombinant mammalian myosin VI. Addition of F-actin to the egg extract to trap myosin VI in the absence of ATP, and subsequent solubilization with ATP effectively concentrated myosin VI. Eleven kinds of myosin mRNAs have been identified in unfertilized sea urchin eggs (*27*) and 12 classes myosin genes have been identified by the *S. purpuratus* Genome Project (*33*). Thus, the ATP-soluble fraction was predicted to contain other classes of myosin. Actually, conventional myosin (myosin II) has been isolated from sea urchin eggs (*34*, *35*), and we detected a 200 kDa band in the ATP soluble fraction, which presumably was myosin II heavy chain. The myosin II-like protein was separated from myosin VI by gel filtration column chromatography due to its larger size, and was not detected in the purified myosin VI

fraction. In addition, most myosin II was separated from myosin VI at the formation of the aggregates with added F-actin: most myosin II remained in the soluble fraction as judged by a western blotting analysis (data not shown). SDS–PAGE analysis showed that the impurities of other proteins were very small in the purified myosin VI fraction, indicating that the amount of other myosin was negligibly small in the final fraction.

Kinetics and Ca^{2+} Regulation of Native Myosin VI—The measurement of actin-activated MgATPase activity revealed the kinetic properties of the native myosin VI. K_{ATP} of the native myosin VI was two or three times larger than that of recombinant mouse myosin VI (*18*). This may indicate that the native myosin VI has an affinity for ATP lower than that of recombinant myosin VI, or that the sea urchin egg myosin VI has it lower than that of mouse myosin VI. As for K_{actin}, the value for the native myosin VI was about 10 times larger than that for recombinant porcine myosin VI as reported previously (*18*), but it was close to the value reported for recombinant mouse myosin VI (*18*). Therefore, the difference in the K_{actin} value between the native sea urchin egg myosin VI and the recombinant porcine myosin VI may not be due to the difference between the native protein and the recombinant one, but may be due to possible difference in the assay conditions, or the animal species, or because we did not use sea urchin egg actin in the assay.

The native myosin VI had an enzymatic property distinct from that reported for the recombinant proteins. The actin-activated MgATPase activity was stimulated by high Ca^{2+} concentrations, whereas the sliding velocity was lowered under the same condition. It has been reported from two laboratories that the MgATPase activity of recombinant mammalian myosin VI was not affected by free Ca^{2+} concentration (*18*, *19*). This is clearly different from our result on the native myosin VI. As to the effect of Ca^{2+} on the sliding velocity on F-actin, the published results are inconsistent with each other: one report has described that the sliding velocity was suppressed at Ca^{2+} concentrations higher than 1 μM only when Thr^{406} is phosphorylated (*18*), while the other has described that the velocity is lowered at high Ca^{2+} concentrations irrespective of phosphorylation at the Thr^{406} (*19*). Although we did not examine whether the native myosin VI is phosphorylated or not, the effect of Ca^{2+} on the sliding velocity was similar to the latter report. The most likely explanation for the difference in the effect of Ca^{2+} on the Mg^{2+}-ATPase activity of native and recombinant myosin VIs is that the recombinant proteins used so far lack the C-terminal globular tail domain, and some steric changes involved in this region in the presence or absence of Ca^{2+} may affect the ATPase activity. The opposite effects of Ca^{2+} on the Mg^{2+}-ATPase activity and the motility have also been seen in both native and recombinant myosin V: the Mg^{2+}-ATPase activity is increased the presence of Ca^{2+} (*36–40*). Myosin V adopts a compact folded conformation in the absence of Ca^{2+} and Ca^{2+} induces an unfolding of the molecule (*37–40*). However, there are differences between myosin VI and V. First, binding of calmodulin was not affected by free Ca^{2+} concentration in myosin VI, while it dissociates from myosin V at high Ca^{2+} concentrations. Second, the activation of ATPase activity of myosin VI by increasing free Ca^{2+} concentration was about 2-fold, while the ATPase activity of myosin V is markedly stimulated. Further study will reveal whether or not Ca^{2+} induces conformational changes in the native myosin VI.

Native Myosin VI is a Monomeric and Non-processive Motor—Myosin VI has been predicted to have a coiled-coil domain between the IQ motif and the globular tail by programs such as COILS (*41*). However, there is a region in this domain where the heptad repeats are not present. It has been reported that myosin VI behaves as a monomeric protein, and speculated that the breakage of the heptad repeats prevents dimerization of the molecule (*16*). Consistent with this report, sea urchin myosin VI also has a region where the heptad repeats are not present in its predicted coiled-coil domain according to amino acid sequence analysis (*27*). Electron microscopy also suggested that the native myosin VI is monomeric. The length of the molecule we measured (54.8 ± 11.3 nm) was longer than that was reported for negatively stained recombinant chicken brush border myosin VI molecules (17 nm) whose tail domain may be folded (*16*). Recently, rotary-shadowed images of recombinant porcine myosin VI molecule have been reported (*17*) and the length of the molecule estimated from the published picture is 35–45 nm. This is still about 15 nm shorter than the length of the native myosin VI. The heavy chain of sea urchin myosin VI is only about 10 aa longer than that of the vertebrate proteins, which may not account for the difference in the length of the molecules. We consider that the recombinant porcine myosin VI was somehow folded while the native sea urchin egg myosin VI was unfolded when prepared for rotary shadowing.

We estimated the sliding velocity of sea urchin egg myosin VI on F-actin at low Ca^{2+} concentrations be 0.2 μm/s. This value was a little lower than the velocity of recombinant mammalian myosin VI [0.3–0.4 μm/s, (*18*, *19*)], but was in the same order. At high Ca^{2+} concentrations the velocity of sea urchin egg myosin VI was lowered to about a half of that at low Ca^{2+} concentrations. Similar effect of Ca^{2+} has been reported for recombinant porcine myosin VI (*19*). On the other hand, movement of recombinant mouse recombinant myosin VI has been reported to be almost inhibited by Ca^{2+} (*18*).

The native myosin VI showed the pointed end-directed movement on F-actin. It has recently been reported that the directionality of sliding of myosin VI is determined by the presence of a unique insert sequence on the motor domain (*15*, *42*). The sea urchin egg myosin VI also has this insert sequence. It is likely that the structure around the insert sequence is preserved on the recombinant proteins.

We examined the processivity of the native myosin VI by estimating both the landing rate of F-actin on the myosin VI-coated glass surface and the duty ratio. Motility assay was performed using the antibodies to tether myosin VI onto nitrocellulose-coated glass coverslips. There is a possibility that myosin VI behaved as dimers or was actually dimerized with its coiled-coil domain if two myosin VI molecules bound to one

IgG molecule. However, the concentration of the antibodies on the cover slips was 5–50 times larger than that of myosin VI tethered by the antibodies, and therefore, it is most likely that one myosin VI molecule bound to one IgG molecule. Thus, it would be reasonable to conclude that myosin VI behaved as a monomeric protein in the present assay conditions, and that the native monomeric myosin VI was a non-processive motor as reported for recombinant myosin VI (*16*).

Localization of Myosin VI in Sea Urchin Eggs—To investigate the function of myosin VI in sea urchin eggs, we examined its localization. The staining pattern by antibodies against myosin VI of unfertilized eggs showed cytosolic punctate distribution. The meaning of this distribution is not clear, but myosin VI could be stored as clusters in the cytoplasm of these quiescent cells. After fertilization, however, myosin VI was translocated to the egg cortex. It has been reported that Ca^{2+} concentration in unfertilized eggs is about 10^{-8} M and transiently increases to 10^{-6} M during fertilization (*43*) and that actin polymerizes in the cortical layer upon fertilization to form a meshwork (*44–48*). It has also been reported that the cortical activity increases after fertilization so that coated pits and coated vesicles are frequently observed in the cortical layer and these structures are associated with actin filaments [(*49–51*); Usukura, J. and Mabuchi, I. unpublished observations]. A majority of the actin filaments are attached to the plasma membrane at their barbed ends (*52*). Myosin VI in the cortex of fertilized eggs may function after the Ca^{2+} concentration returns to the resting level (*43*), since its F-actin sliding activity is high at low Ca^{2+} concentrations, and may be needed for endocytic vesicles to pass through the dense actin meshwork using its property to move toward the pointed end of F-actin as reported in mammalian cultured cell (*13*). During cleavage, the contractile ring is formed in the cleavage furrow (*29*, *43*, *53*). Myosin VI was concentrated in the contractile ring region. This is similar to the finding that myosin VI is present in the metaphase furrow in *Drosophila* embryos and thought to transport components required for furrow formation (*5*). It is tempting to speculate that myosin VI is required for contractile ring formation or membrane addition during cleavage in sea urchin eggs.

We are grateful to Dr Megumi Moriya (Hokkaido Univ., Sapporo) for the gift of the antibody against calmodulin. We also thank Dr. Yoko Toyoshiman the member of Mabuchi lab for helpful discussions. This study was supported by a research grant from the JSPS (#15207013).

REFERENCES

1. Hodge, T. and Cope, M.J. (2000) A myosin family tree. *J. Cell Sci.* **113**, 3353–3354
2. Kellerman, K.A. and Miller, K.G. (1992) An unconventional myosin heavy chain gene from *Drosophila melanogaster*. *J. Cell Biol.* **119**, 823–834
3. Avraham, K.B., Hasson, T., Steel, K.P., Kingsley, D.M., Russell, L.B., Mooseker, M.S., Copeland, N.G., and Jenkins, N.A. (1995) The mouse *Snell's waltzer* deafness gene encodoes an unconventional myosin required for structural integrity of inner ear hair cells. *Nat. Genet.* **11**, 369–375
4. Hasson, T. and Mooseker, M.S. (1994) Porcine myosin-VI: Characterization of a new mammalian unconventional myosin. *J. Cell Biol.* **127**, 425–440
5. Mermall, V. and Miller, K.G. (1995) The 95F unconventional myosin is requaired for proper organization of the *Drosophila* syncytial blastderm. *J. Cell Biol.* **129**, 1575–1588
6. Hicks, J.L., Deng, W.M., Rogat, A.D., Miller, K.G., and Bownes, M. (1999) Class VI unconventional myosin is required for spermatogenesis in *Drosophila*. *Mol. Biol. Cell* **10**, 4341–4353
7. Noguchi, T., Lenartowska, M., and Miller, K.G. (2006) Myosin VI stabilizes an actin Network during *Drosophila* spermatid individualization. *Mol. Biol. Cell* **17**, 2559–2571
8. Self, T., Sobe, T., Copeland, N.G., Jenkins, N.A., Avraham, K.B., and Steel, K.P. (1999) Role of myosin VI in the differentiation of cochlear hair cells. *Dev. Biol.* **214**, 331–341
9. Buss, F., Arden, S.D., Lindsay, M., Luzio, J.P., and Kendrick-Jones, J. (2001) Myosin VI isoform localized to clathrin-coated vesicles with a role in clathrin-mediated endocytosis. *EMBO J.* **20**, 3676–3684
10. Aschenbrenner, L., Lee, T., and Hasson, T. (2003) Myo6 facilitates the translocation of endocytic vesicles from cell peripheries. *Mol. Biol. Cell* **14**, 2728–2743
11. Morris, S.M., Arden, S.D., Roberts, R.C., Kendrick-Jones, J., Cooper, J.A., Luzio, J.P., and Buss, F. (2002) Myosin VI binds to and localises with Dab2, potentially linking receptor-mediated endocytosis and the actin cytoskeleton. *Traffic* **3**, 331–341
12. Wells, A.L., Lin, A.W., Chen, L.Q., Safer, D., Cain, S.M., Hasson, T., Carragher, B.O., Milligan, R.A., and Sweeney, H.L. (1999) Myosin VI is an actin-based motor that moves backwards. *Nature* **401**, 505–508
13. Aschenbrenner, L., Naccache, S.N., and Hasson, T. (2004) Uncoated endocytic vesicles require the unconventional myosin, Myo6, for rapid transport through actin barriers. *Mol. Biol. Cell* **15**, 2253–2263
14. Bahloul, A., Chevreux, G., Wells, A.L., Martin, D., Nolt, J., Yang, Z., Chen, L.-Q., Potier, N., Dorsselaer, A.V., Rosenfeld, S., Houdusse, A., and Sweeney, H.L. (2004) The unique insert in myosin VI is a structural calcium-calmozdulin binding site. *Proc. Natl Acad. Sci. USA* **101**, 4787–4792
15. Ménétrey, J., Bahloul, A., Wells, A.L., Yengo, C.M., Morris, C.A., Sweeney, H.L., and Houdusse, A. (2005) The structure of the myosin VI motor reveals the mechanism of directionality reversal. *Nature* **435**, 779–785
16. Lister, I., Schmitz, S., Walker, M., Trinick, J., Buss, F., Veigel, C., and Kendrick-Jones, J. (2004) A monomeric myosin VI with a large working stroke. *EMBO J.* **23**, 1729–1738
17. Park, H., Ramamurthy, B., Travaglia, M., Safer, D., Chen, L.-Q., Franzini-Aemstrong, C., Selvin, P.R., and Sweeney, H.L. (2006) Full-length myosin VI dimerizes and moves processively along actin filaments upon monomer clustering. *Mol. Cell* **21**, 331–336
18. Yoshimura, M., Homma, K., Saito, J., Inoue, A., Ikebe, R., and Ikebe, M. (2001) Dual regulation of myosin VI motor function. *J. Biol. Chem.* **276**, 39600–39607
19. Morris, C.A., Wells, A.L., Yang, Z., Chen, L.-Q., Baldacchino, C.V., and Sweeney, H.L. Calcium functionally uncouples the heads of myosin VI. *J. Biol. Chem.* 278, 23324–23330
20. Terasaki, A.G., Ohnuma, M., and Mabuchi, I. (1997) Identification of actin-binding proteins from sea urchin eggs by F-actin affinity column chromatography. *J. Biochem.* **122**, 226–236
21. Weeds, A.G. and Hartley, B.S. (1968) Selective purification of the thiol peptides of myosin. *Biochem. J.* **107**, 531–548
22. Spudich, J.A. and Watt, S. (1971) The regulation of rabbit skeletal muscle contraction.I. Biochemical studies of the

interaction of the tropomyosin-troponin complex with actin and proteolytic fragments of myosin. *J. Biol. Chem.* **246**, 4866–4871
23. Kodama, T., Fukui, K., and Kometani, K. (1986) The initial phosphate burst in ATP hydrolysis by myosin and subfragment-1 as studied by a modified Malachite Green method for determination of inorganic phosphate. *J. Biochem.* **99**, 1465–1472
24. Kron, S.J. and Spudich, J.A. (1986) Fluorescent actin filaments move on myosin fixed to a glass surface. *Proc. Natl Acad. Sci. USA* **83**, 6272–6276
25. Hancock, W.O. and Howard, J. (1998) Processivity of the motor protein kinesin requires two heads. *J. Cell Biol.* **40**, 1395–1405
26. Uyeda, T., Kron, S., and Spudich, J.A. (1990) Myosin step size estimation from slow sliding movement of actin over low densities of heavy meromyosin. *J. Mol. Biol.* **214**, 699–710
27. Sirotkin, V., Speipel, S., Krendel, M., and Bonder, E.M. (2000) Characterization of sea urchin unconventional myosins and analysis of their patterns of expression during early embryogenesis. *Mol. Reprod. Dev.* **57**, 111–126
28. Hirako, Y., Usukura, J., Uematsu, J., Hashimoto, T., Kitajima, Y., and Owaribe, K. (1998) Cleavage of BP180, a 180-kDa bullous pemohigoid antigen, yields a 120-kDa collagenous extracellular polypeptide. *J. Biol. Chem.* **273**, 9711–9717
29. Mabuchi, I. (1994) Cleavage furrow: timing of emergence of contractile ring actin filaments and establishment of the contractile ring by filament bundling in sea urchin eggs. *J. Cell Sci.* **107**, 1853–1862
30. Swanljung-Collins, H. and Collins, J.H. (1991) Ca^{2+} stimulates the Mg^{2+}-ATPase activity of brush border myosin I with three or four calmodulin light chains but inhibits with less than two bound. *J. Biol. Chem.* **266**, 1312–1319
31. Homma, K., Saito, J., Ikebe, R., and Ikebe, M. (2000) Ca^{2+}-dependent regulation of the motor activity of myosin V. *J. Biol. Chem.* **275**, 34766–34771
32. Rock, R.S., Rice, S.E., Wells, A.L., Purcell, T.J., Spudich, J.A., and Sweeney, H.L. (2001) Myosin VI is a processive motor with a large step size. *Proc. Natl Acad. Sci. USA* **98**, 13655–13659
33. Morris, R.L., Hoffman, M.P., Ober, R.A., McCafferty, S.S., Gibbons, I.R., Leone, A.D., Cool, J, Allgood, E.L., Musante, A.M., Judkins, K.M., Rossetti, B.J., Rawson, A.P., and Burgess, D.R. (2006) Analysis of cytoskeletal and motility proteins in the sea urchin genome assembly. *Dev. Biol.* **300**, 219–237
34. Mabuchi, I. (1973) A myosin-like protein in the cortical layer of the sea urchin egg. *J. Cell Biol.* **59**, 542–547
35. Kane, R.E. (1983) Interconversion of structual and contractile actin-based gels by insertion of myosin during assembly. *J. Cell Biol.* **97**, 1745–1752
36. Cheney, R.E., O'Shea, M.K., Heuser, J.E., Coelho, M.V., Wolenski, J.S., Espreafico, E.M., Forscher, P., Larson, R.E., and Mooseker, M.S. (1993) Brain myosin-V is a two-headed unconventional myosin with motor activity. *Cell* **75**, 12–23
37. Krementsov, D.N., Krementsova, E.B., and Trybus, K.M. (2004) Myosin V: regulation by calcium, calmodulin, and the tail domain. *J. Cell Biol.* **164**, 877–886
38. Li, X.-D., Mabuchi, K., Ikebe, R., and Ikebe, M. (2003) Ca^{2+}-induced activation of ATPase activity of myosin Va is accompanied with a large conformational change. *Biochem. Biophys. Res. Comm.* **315**, 538–545
39. Wang, F., Thirumurugan, K., Stafford, W.F., Hammer III, J.A., Knight, P.J., and Sellers, J.R. (2004) Regulated conformation of myosin V. *J. Biol. Chem.* **279**, 2333–2336
40. Thirumurugan, K., Sakamoto, T., Hammer III, J.A., Sellers, J.R., and Knight, P.J. (2006) The cargo-binding domain regulates structure and activity of myosin 5. *Nature* **442**, 212–215
41. Lupas, A. (1996) Prediction and analysis of coiled-coil structures. *Method Enzymol* **266**, 513–525
42. Bryant, Z., Altman, D., and Spudich, J.A. (2006) The power stroke of myosin VI and the basis of reverse directionality. *Proc. Natl Acad. Sci. USA* **104**, 772–777
43. Poenie, M., Alderton, J., Tsien, R.Y., and Steinhardt, R.A. (1985) Change of free calcium levels with stages of the cell division cycle. *Nature* **315**, 147–149
44. Mabuchi, I., Hosoya, H., and Sakai, H. (1980) Actin in the cortical layer of the sea urchin egg: changes in its content during and after fertilization. *Biomed. Res.* **1**, 417–426
45. Yonemura, S. and Kinoshita, S. (1986) Actin filament organization in the sand dollar egg cortex. *Dev. Biol.* **115**, 171–183
46. Spudich, A. and Spudich, J.A. (1979) Actin in triton-treated cortical preparations of unfertilized and fertilitzed sea urchin eggs. *J. Cell Biol.* **82**, 212–226
47. Yonemura, S. and Mabuchi, I. (1987) Wave of cortical actin in the sea urchin egg. *Cell Motil. Cytoskeleton* **7**, 46–53
48. Hamaguchi, Y. and Mabuchi, I. (1988) Accumulation of fluorescently labeled actin in the cortical layer in sea urchin eggs after fertilization. *Cell Motil. Cytoskeleton* **9**, 153–163
49. Rebhun, L.I. and Fisher, G.W. (1984) Initiation of two-way cortical traffic after fertilization in sea urchin eggs. *J. Cell Biol.* **99**, 129s–131s
50. Chandler, D.E. and Heuser, J. (1979) Membrane fusion during secretion: cortical granule exocytosis in sea urchin eggs as studied by quick-freezing and freeze-fracture. *J. Cell Biol.* **83**, 91–108
51. Whalley, T., Terasaki, M., Cho, M.S., and Vogel, S.S. (1995) Direct membrane retrieval into large vesicles after exocytosis in sea urchin eggs. *J. Cell Biol.* **131**, 1183–1192
52. Ishidate, S. and Mabuchi, I. (1988) Localization and possible function of 20kDa actin-modulating protein(actolinkin) in the sea urchin egg. *Eur. J. Cell Biol.* **46**, 275–281
53. Schroeder, T.E. (1973) Actin in dividing cells: contractile ring filaments bind heavy meromyosin. *Proc. Natl Acad. Sci. USA* **70**, 1688–1692